厚生労働科学補助金（創薬基盤推進研究事業）分担研究報告

「難治がんの創薬バイオマーカー探索研究」

氏名	所属	職名
分担研究者　近藤格	国立がんセンター研究所	
プロテオーム・バイオインフォマティクス・プロジェクト		リーダー

研究要旨

創薬バイオマーカー探索のために、蛍光二次元電気泳動法を用いて肝細胞癌症例における腫瘍組織と非腫瘍組織の間で発現差のあるタンパク質を同定するための試料調整を行った。国立がんセンター中央病院で手術を受けた肝細胞癌の４３症例から得られた８６検体（腫瘍組織４３検体、非腫瘍組織４３検体）よりタンパク質を抽出し、濃度測定と品質チェックを行った。濃度測定と容量測定の結果、蛍光二次元電気泳動法を行うのに必要な量のタンパク質が８４検体（腫瘍組織４２検体、非腫瘍組織４２検体）より回収できていることが確認された。プロテオーム解析を阻害するような激しい血清タンパク質のコンタミはSDS-PAGEのレベルでは確認できなかった。数および品質の点から、回収されたタンパク質サンプルを用いたプロテオーム解析を行うことが可能であることが分かった。

A.　研究目的

肝細胞癌は本邦では悪性腫瘍死の第４位を占める。肝細胞癌の５年生存率は40%程度と不良である。治療成績の向上を目指した診断法と治療法の開発が行われている。

肝細胞癌症例において腫瘍組織と非腫瘍組織の間で発現差を示すタンパク質は診断のためのバイオマーカー候補であると同時に、創薬のための分子標的とみなすことができる。そのようなタンパク質を探索する試みは過去に盛んに行われており、多数の論文が発表されている。しかしながら、多くの場合は十分な数の症例数において研究が行われていないこと、同定されたタンパク質の臨床応用が本格的に行われていなかったことから、同定されたタンパク質の臨床応用にはいたっていない。

本研究では国立がんセンターで開発されたプロテオーム解析の技術と、同センターで手術を受けた肝細胞癌症例の手術検体を用いたプロテオーム解析を行い、診断技術や創薬に有用なタンパク質の同定を行うことを目的とする。

B. 研究方法

国立がんセンター中央病院にて手術を受けた肝細胞癌８４症例を対象とし、切除され保管されていた手術検体を使用した。

タンパク質抽出の目的で組織検体を液体窒素の存在下で破砕し粉末状にした。次に高濃度のウレアを含むタンパク質可溶化液を使って粉末状になった組織検体からタンパク質を抽出した。１５０００回転で遠心して上精を回収し、タンパク質サンプルとした。

タンパク質の濃度測定にはブラッドフォード法を用いた。タンパク質サンプルの品質検定にはSDS-PAGE法を用いた。

（倫理面への配慮）

国立がんセンターの倫理委員会による審査で承認された方法で採取保管され、検体の個人情報が漏出することが無いように匿名化が厳重に行われるように配慮したがん患者の手術検体を用いた。

C、研究結果

合計８６検体（腫瘍組織４３検体、非腫瘍組織４３検体）からタンパク質の抽出を試みたところ、蛍光二次元電気泳動法を実施するために必要な量のタンパク質が８４検体（腫瘍組織４２検体、非腫瘍組織４２検体）から回収できた。SDS-PAGEにて5μgのタンパク質を分離して観察したところ、プロテオーム解析を阻害するような激しい血清タンパク質のコンタミは確認されなかった。

D. 考察

合計８４検体より十分な量のタンパク質サンプルを得ることができた。品質についてはSDS-PAGEで確認できるような激しい血清タンパク質のコンタミはなかったことから、このまま蛍光二次元電気泳動法を用いたプロテオーム解析を開始することを計画している。

E，結論

計画している肝細胞癌のプロテオーム解析のための試料調整を行うことができた。今回の実験で得られたタンパク質サンプルを使って平成２１年度はプロテオーム解析を行う。

F，健康危険情報

特になし

G，研究発表

1. 論文発表

1. Kikuta K, Tochigi N, Shimoda T, Yabe H, Morioka H, Toyama Y, Hosono A, Beppu Y, Kawai A, Hirohashi S, Kondo T, Nucleophosmin as a candidate prognostic biomarker of Ewing sarcoma revealed by proteomics. Clin Cancer Res, in press
2. Yamada M, Fujii K, Koyama K, Hirohashi S, Kondo T, The proteomic profile of pancreatic cancer cell lines corresponding to carcinogenesis and metastasis. J Proteomics Bioinform, 2, 1-18, 2009

3. Kondo T, Tissue proteomics for cancer biomarker development: laser microdissection and 2D-DIGE. BMB Rep, 41, 626-34, 2008
4. Kondo T, Cancer proteomics for biomarker development. J Proteomics Bioinform, 1, 477-84, 2008
5. Uemura N, Nakanishi Y, Kato H, Saito S, Nagino M, Hirohashi S, Kondo T, Transglutaminase 3 as a prognostic biomarker in esophageal cancer revealed by proteomics. Int J Cancer, 124, 2106-15, 2009
6. Saito S, Ojima H, Ichikawa H, Hirohashi S, Kondo T, Molecular background of alpha-fetoprotein in liver cancer cells as revealed by global RNA expression analysis. Cancer Sci, 99, 2402-9, 2008
7. Orimo T, Ojima H, Hiraoka N, Saito S, Kosuge T, Kakisaka T, Yokoo H, Nakanishi K, Kamiyama T, Todo S, Hirohashi S, Kondo T, Proteomic profiling reveals the prognostic value of adenomatous polyposis coli-end-binding protein 1 in hepatocellular carcinoma. Hepatology, 48, 1851-63, 2008
8. Kawai A, Kondo T, Suehara Y, Kikuta K, Hirohashi S, Global protein-expression analysis of bone and soft tissue sarcomas. Clin Orthop Relat Res, 466, 2099-106, 2008
9. Pfetin as a prognostic biomarker of gastrointestinal stromal tumors revealed by proteomics. Clin Cancer Res, 14, 1707-17, 2008

2．学会発表

1. Human Proteome Organization年会、オランダアムステルダム市、Tadashi Kondo et al. Cancer Proteomics for Personalized Medicine
2. 日本プロテオーム機構年会、大阪、Tadashi Kondo, Cancer Biomarker Discovery for Personalized Medicine
3. 韓国プロテオーム機構年会、韓国済州島、Tadashi Kondo, Cancer Proteomics for Personalized Medicine
4. Asia-Oceania Human Proteome Organization年会、オーストラリアケアンズ市、Tadashi Kondo, Cancer Proteomics for Personalized Medicine
5. HongKong Human Proteome Organization年会, 中華人民共和国香港、Tadashi Kondo, Cancer Proteomics for Biomarker Development
6. Taiwan-Japan Joint Symposium, Taiwan Proteome Society年会、Tadashi Kondo, Cancer Proteomics for Biomarker Development

H．知的財産権の出願・登録状況（予定を含む）

1.特許出願

国内出願

「食道癌の予後予測方法」特願2008-278554

国際出願

1. 「消化管間質腫瘍（GIST）を処置するための医薬組成物、ならびに消化管間質腫瘍を患う患者の予後を予測するためのキットおよび方法」PCT/JP2008/71495
2. 「肝細胞癌のマーカーおよび肝細胞癌の検査方法」PCT/JP2008/

71495

2.実用新案登録

特記事項なし

3.その他

特記事項なし

厚生労働科学補助金（創薬基盤推進研究事業）分担研究報告

「難治がんの創薬バイオマーカー探索研究」

	氏名	所属	職名
分担研究者	中山敬一	九州大学生体防御医学研究所	教授

研究要旨

生体内で起きているリン酸化は極めてダイナミックに変化するため、その変化を定量的にモニターすることは重要である。質量分析を用いたタンパク質の網羅的定量法としてはこれまでSILAC法やICAT法が知られているが、時系列での変動を調べるためには４点（あるいは８点）での定量解析が可能であるiTRAQ法は非常に魅力的である。その一方で、ペプチドの化学標識を必要とするiTRAQ法は複雑な操作による定量エラーが起きやすく、真の変化と実験誤差による変化を見極めることは難しい。本研究ではより信頼性の高いリン酸化ペプチドのiTRAQ法による定量解析法の確立を目指し、システムの確立を行った。臨床検体の解析にこの手法を導入することで難治がんの創薬に対する新規バイオマーカーの開発が促進されることが期待される。

A. 研究目的

リン酸化ペプチドの精製は質量分析計によるリン酸化部位の同定のためには欠かすことのできない技術である。近年、金属アフィニティークロマトグファフィーや酸化チタンを用いたリン酸化ペプチドの精製技術が確立され、おもにSILAC法を用いた定量リン酸化プロテオーム解析がいくつか報告されている。SILAC法の最大の利点は以前にも述べたように標識後の細胞や抽出物を混合した後に酵素消化や精製操作を行えることである、そのため基本的には試料を混合するときのタンパク質量がそろっていれば、その後の操作で生じるエラーは異なる試料間で全く同じになるはずである。一方、iTRAQ法は酵素消化のあとにしか標識することができない。また、リン酸化ペプチドをIMACなどで精製する場合は、標識したペプチドを混合してから精製することが実験誤差を減らすために理想的であるが、ラベル剤のコストを考慮すると最初に使用するタンパク質量に制限が生じる。具体的には現在のわれわれの方法では100 μgの消化物から同定できるリン酸化ペプチドは500-1000種類程度であり、同定数を倍に上げるにはその10倍以上のタンパク質が必要であ

る。iTRAQ 試薬は 1 バイアルで 100 μg 消化物を標識できるように設定されており、1 mg のタンパク質を標識するためには 10 バイアルを消費することになる。われわれは数千から 1 万種類のリン酸化を検出することを目的としており、これを達成するには 4~5 mg ほどのペプチドを標識することになり、IMAC 前の標識は現実的ではない。

このような理由からリン酸化の大規模定量解析のためには IMAC 後の iTRAQ 標識が現実的にはただ一つの選択肢となる。しかしながら、前述したように標識前の複雑な操作は多くの誤差を生じさせる可能性が高い。操作中に生じた回収量のブレはそのまま定量値に反映されてしまうため、そのデータをもとにしたその後の研究に致命的な影響を及ぼしかねない。そのようなエラーを防ぐためには実験を複数回繰り返して再現性を得ることが重要であるが、時間・労力・高価な試薬を要する大規模解析を何度も繰り返すことは現実的ではない。したがって、一回の実験の信頼性をどの程度まで上げられるかが重要な課題となる。このような理由から、われわれはリン酸化ペプチドの定量解析に iTRAQ を導入する際、IMAC のキャパシティーや精製の定量性の詳細な検討を行っている。さらに、内部標準リン酸化タンパク質を試料に添加することで、実験過程で生じるブレを補正することも可能になってきた。本研究ではタンパク質のリン酸化を大規模に多点定量するための方法論の確立と実際の難治がんの創薬に対する新規バイオマーカー探索への応用の可能性を探索した。

B. 研究方法

HeLa 細胞抽出物を 4 つのチューブに分注(1 mg/tube)し、各々に 2.5, 5, 10, 20 ug の bovine casein および chick ovalbumin を添加した（われわれの実験系では主にヒトあるいはマウスの試料を用いることが多いのでこの二つのタンパク質を選定しており、HeLa 細胞由来のペプチドと識別可能である)。これらの試料をトリプシン消化し、脱塩後、IMAC によるリン酸化ペプチドの精製を行った。得られたリン酸化ペプチドをそれぞれ 114, 115, 116, 117 の iTRAQ 試薬で標識し、混合した。1/20 量の標識ペプチドを遠心濃縮し、0.5% TFA に再溶解後、STAGE tip にて脱塩を行った。再度遠心濃縮した後、0.1% TFA/2%アセトニトリルに溶かして 1/2 量を QSTAR elite にて分析した。

（倫理面への配慮）

本研究においてはヒトサンプルを扱っておらず、特に倫理面に関する問題点はない。

C、研究結果

Casein や OVA 由来のリン酸化ペプチドの MS/MS スペクトルのおいて観測

されるリポーターイオンの強度比はほぼ理論値と一致した。その平均を図２に示す。一方、HeLa 細胞由来のリン酸化ペプチドの定量値はほぼ１に収束していた。これらの結果は複雑な混合物に含まれる量比が異なるリン酸化タンパク質は消化や IMAC 精製、さらには iTRAQ 標識のプロセスを経ても定量的に回収され、その存在比を iTRAQ 法にてほぼ正確に定量可能であることが判明した。

上述したように IMAC 後に iTRAQ 標識を行っても定量性は確保できることが分ったが、複雑な課程を含む実験にブレはつきものである。特に、まったくの未知試料での分析では定量値に偏りが生じた場合、それが真の値なのか実験誤差によるものなのかの判断は非常に難しい。そこで、われわれは比較したい試料に既知量の評品リン酸化タンパク質(bovine casein や chick ovalbumin)をスパイクすることで実験の過程で生じる誤差をモニターすることを考案した。最終的に得られる iTRAQ での定量結果は内部標準タンパク質由来のリン酸化ペプチドの実測定量値（本来は一定量ずつ加えているので定量値は1:1:1:1となるはずである）を用いて全体の定量値を補正できる。消化前の段階でスパイクしておけば変性の度合、消化効率、カラム流速などのバラつき、さらには iTRAQ 試薬の標識効率などのすべての過程で生じた誤差を最終的に補正可能である。実例を示すが、1 mg の HeLa 細胞抽出液に一定量(HeLa 細胞抽出液の0.05%に相当)の評品リン酸化タンパク質（bovine casein と chick ovalbumin）を添加してから、一連のリン酸化ペプチド精製プロトコルを実行した。評品リン酸化タンパク質の定量値に若干のばらつきがあった。

D. 考察

今回、iTRAQ 法を用いた大規模なリン酸化の変動解析のために新しい技術基盤を確立した。これまでに報告されているリン酸化の大規模定量解析のほとんどが SILAC 法を用いて行われている。定量ポイントの多さや出発試料を選ばないことから iTRAQ 法のリン酸化ペプチド定量解析への適用は非常に魅力的であるが、普及が進んでいないのが実情である。その理由は試薬のコストによる実験系の制限、その結果生じる実験系の複雑さによる定量エラーのリスクがあげられる。しかしながら、慎重に実験を行えば IMAC の定量エラーは最小限にとどめることが可能であるし、たとえエラーが生じても、内部標準を用いた補正で信頼性を回復できることがわかった。今後、iTRAQ 法は様々なプロテオミクスのアプリケーションに取り入れられる定量法となることが十分に期待される。

E. 結論

質量分析による定量的プロテオミクスである iTRAQ 法を用いてリン酸化タンパク質を定量するという

phospho-iTRAQ法技術の基盤を確立した。

F. 健康危険情報

特になし

G. 研究発表

1. 論文発表

1. Matsuoka, S., Oike, Y., Onoyama, I., Iwama, A., Arai, F., Takubo, K., Mashimo, Y., Oguro, H., Nitta, E., Ito, K., Miyamoto, K., Yoshiwara, H., Hosokawa, K., Nakamura, Y., Gomei, Y., Iwasaki, H., Hayashi, Y., Matsuzaki, Y., Nakayama, K., Ikeda, Y., Hata, A., Chiba, S., Nakayama, K. I., Suda, T.: Fbxw7 acts as a critical fail-safe against premature loss of hematopoietic stem cells and development of T-ALL. ***Genes Dev.***, 22: 986-991 (2008).
2. Inoue, S., Kinoshita, T., Matsumoto, M., Nakayama, K. I., Doi, M., Shimazaki, K.: Blue light-induced autophosphorylation of phototropin is a primary step for signaling. ***Proc. Natl. Acad. Sci. U S A***, 105: 5626-5631 (2008).
3. Mukai, A., Mizuno, E., Kobayashi, K., Matsumoto, M., Nakayama, K. I., Kitamura, N., Komada, M.: Dynamic regulation of ubiquitylation and deubiquitylation at the central spindle during cytokinesis. ***J. Cell Sci.***, 121: 1325-1333 (2008).
4. Song, M. S., Song, S. J., Kim, S. J., Nakayama, K., Nakayama, K. I., Lim, D. S.: Skp2 regulates the antiproliferative function of the tumor suppressor RASSF1A via ubiquitin-mediated degradation at the G1-S transition. ***Oncogene***, 27: 3176-3185 (2008).
5. Shigematsu, N., Fukuda, T., Yamamoto, T., Nishioku, T., Yamaguchi, T., Himeno, M., Nakayama, K. I., Tsukuba, T., Kadowaki, T., Okamoto, K., Higuchi, S., Yamamoto, K.: Association of cathepsin E deficiency with the increased territorial aggressive response of mice. ***J. Neurochem.***, 105: 1394-1404 (2008).
6. Chen, Q., Xie, W., Kuhn, D. J., Voorhees, P. M., Lopez-Girona, A., Mendy, D., Corral, L. G., Krenitsky, V. P., Xu, W., Moutouh-de Parseval, L., Webb, D. R., Mercurio, F., Nakayama, K. I., Nakayama, K., Orlowski, R. Z.: Targeting the p27 E3 ligase SCF^{Skp2} results in p27- and Skp2-mediated cell-cycle arrest and activation of autophagy. ***Blood***, 111: 4690-4699 (2008).
7. Shirane, M., Ogawa, M., Motoyama, J., Nakayama, K. I.: Regulation of apoptosis and neurite extension by FKBP38 is required for neural tube formation in the mouse. ***Genes Cells***, 13: 635-651 (2008).

8. Agarwal, A., Bumm, T. G., Corbin, A. S., O'Hare, T., Loriaux, M., VanDyke, J., Willis, S. G., Deininger, J., Nakayama, K. I., Druker, B. J., Deininger, M. W.: Absence of SKP2 expression attenuates BCR-ABL-induced myeloproliferative disease. ***Blood***, 112: 1960-1970 (2008).
9. Matsumoto, A., Kawamoto, T., Mutoh, F., Isse, T., Oyama, T., Kitagawa, K., Nakayama, K. I., Ichiba, M.: Effects of 5-week ethanol feeding on the liver of aldehyde dehydrogenase 2 knockout mice. ***Pharmacogenet. Genomics***, 18: 847-852 (2008).
10. Sakae, N., Yamasaki, N., Kitaichi, K., Fukuda, T., Yamada, M., Yoshikawa, H., Hiranita, T., Tatsumi, Y., Kira, J., Yamamoto, T., Miyakawa, T., Nakayama, K. I.: Mice lacking the schizophrenia-associated protein FEZ1 manifest hyperactivity and enhanced responsiveness to psychostimulants. ***Hum. Mol. Genet.***, 17: 3191-3203 (2008).
11. Ishikawa, Y., Onoyama, I., Nakayama, K. I., Nakayama, K.: Notch-dependent cell cycle arrest and apoptosis in mouse embryonic fibroblasts lacking Fbxw7. ***Oncogene***, 27: 6164-6174 (2008).
12. Ohsaki, K., Oishi, K., Kozono, Y., Nakayama, K., Nakayama, K. I., Ishida, N.: The role of β-TrCP1 and β-TrCP2 in circadian rhythm generation by mediating degradation of clock protein PER2. ***J. Biochem.***, 144: 609-618 (2008).
13. Kanei-Ishii, C., Nomura, T., Takagi, T., Watanabe, N., Nakayama, K. I., Ishii, S.: Fbxw7 acts as an E3 ubiquitin ligase that targets c-Myb for nemo-like kinase (NLK)-induced degradation. ***J. Biol. Chem.***, 283: 30540-30548 (2008).
14. Miranda-Carboni, G. A., Krum, S. A., Yee, K., Nava, M., Deng, Q. E., Pervin, S., Collado-Hidalgo, A., Galic, Z., Zack, J. A., Nakayama, K., Nakayama, K. I., Lane, T. F.: A functional link between Wnt signaling and SKP2-independent p27 turnover in mammary tumors. ***Genes Dev.***, 22: 3121-3134 (2008).
15. Tamamori-Adachi, M., Takagi, H., Hashimoto, K., Goto, K., Hidaka, T., Koshimizu, U., Yamada, K., Goto, I., Maejima, Y., Isobe, M., Nakayama, K. I., Inomata, N., Kitajima, S.: Cardiomyocyte proliferation and protection against post-myocardial infarction heart failure by cyclin D1 and Skp2 ubiquitin ligase. ***Cardiovasc. Res.***, 80: 181-190 (2008).
16. Minhajuddin, M., Bijli, K. M., Fazal, F., Sassano, A., Nakayama, K. I., Hay, N., Platanias, L. C., Rahman, A.: Protein kinase Cδ and PI3-kinase/Akt activate mammalian target of rapamycin to modulate NF-κB activation and ICAM-1 expression in

endothelial cells. ***J. Biol. Chem.***, 284: 4052-4061 (2009).

17. Mitra, P., Ghule, P. N., van der Deen, M., Medina, R., Xie, R. L., Holmes, W. F., Ye, X., Nakayama, K. I., Harper, J. W., Stein, J. L., Stein, G. S., van Wijnen, A. J.: CDK inhibitors selectively diminish cell cycle controlled activation of the histone H4 gene promoter by p220(NPAT) and HiNF-P. ***J. Cell Physiol.***, 219: 438-448 (2009).
18. Tsukuba, T., Yanagawa, M., Okamoto, K., Okamoto, Y., Yasuda, Y., Nakayama, K. I., Kadowaki, T., Yamamoto, K.: Impaired chemotaxis and cell adhesion due to decrease in several cell-surface receptors in cathepsin E-deficient macrophages. ***J. Biochem.***, in press. (2009).
19. Lu, Y., Adegoke, O. A., Nepveu, A., Nakayama, K. I., Bedard, N., Cheng, D., Peng, J., Wing, S. S.: USP19 deubiquitinating enzyme supports cell proliferation by stabilizing KPC1, a ubiquitin ligase for p27Kip1. ***Mol. Cell. Biol.***, 29: 547-558 (2009).
20. Nishiyama, M., Oshikawa, K., Tsukada, Y., Nakagawa, T., Iemura, S., Natsume, T., Fan, Y., Kikuchi, A., Skoultchi, A. I., Nakayama, K. I.: CHD8 suppresses p53-mediated apoptosis through histone H1 recruitment during early embryogenesis. ***Nat. Cell Biol.***, 11: 172-182 (2009).
21. Minhajuddin, M., Bijli, K. M., Fazal, F., Sassano, A., Nakayama, K. I., Hay, N., Platanias, L. C., Rahman, A.: Protein kinase C-{delta} and phosphatidylinositol 3-kinase/Akt activate mammalian target of rapamycin to modulate NF-{kappa}B activation and intercellular adhesion molecule-1 (ICAM-1) expression in endothelial cells. ***J. Biol. Chem.***, 284: 4052-4061 (2009).
22. Endo, A., Matsumoto, M., Inada, T., Yamamoto, A., Nakayama, K. I., Kitamura, N., Komada, M.: Nucleolar structure and function are regulated by the deubiquitylating enzyme USP36. ***J. Cell Sci.***, 122: 678-686 (2009).
23. Susaki, E., Nakayama, K., Yamasaki, L., Nakayama, K. I.: Common and specific roles of the related CDK inhibitors p27 and p57 revealed by a knock-in mouse model. ***Proc. Natl. Acad. Sci. U S A***, in press. (2009).

2. 学会発表

1. Nakayama, K.I.: Epigenetic control of p53 function by CHD8 through recruitment of histone H1. ***The Third International Workshop on Cell Regulations in Division and Arrest Under Stress***. (Invited speaker) Onna, Okinawa, Japan. 4/9 (2008).
2. Ishikawa, Y., Onoyama, I., Okuyama, R., Nakayama, K.I., Nakayama, K.:

Differential specificity of substrate accumulation in ubiquitin ligase SCF^{Fbxw7} deficient fibroblasts and keratinocytes. ***Cold Spring Harbor Symposium "The Cell Cycle"***. Cold Spring Harbor, NY. 5/15 (2008).

3. Susaki, E., Nakayama, K., Nakayama, K.I.: A p27-p57 knock-in mouse model uncovers common and specific roles of p27 and p57. ***Cold Spring Harbor Symposium "The Cell Cycle"***. Cold Spring Harbor, NY. 5/16 (2008).
4. Nishiyama, M., Tsukada, Y.-i., Oshikawa, K., Nakagawa, T., Nakayama, K.I.: Epigenetic control of p53 function by CHD8 through recruitment of histone H1. ***Cold Spring Harbor Symposium "The Cell Cycle"***. Cold Spring Harbor, NY. 5/16 (2008).
5. Matsumoto, A., Onoyama, I., Matsuoka, S., Oike, Y., Suda, T., Nakayama, K.I.: Fbxw7 is essential for G0 maintenance and functions of the stem cells. ***Cold Spring Harbor Symposium "The Cell Cycle"***. Cold Spring Harbor, NY. 5/16 (2008).
6. Matsumoto, M., Oyamada, K., Nakayama, K.I.: A global map of mitotic phosphoproteome uncovers unexpected signaling pathways in mitosis. ***Cold Spring Harbor Symposium "The Cell Cycle"***. Cold Spring Harbor, NY. 5/16 (2008).
7. Nakayama, K.I., Onoyama, I., Tsunematsu, R., Matsumoto, A., Nakayama, K.: Conditional inactivation of Fbxw7 results in a defect in cell cycle exit and tumorigenesis. ***Cold Spring Harbor Symposium "The Cell Cycle"***. (Invited speaker) Cold Spring Harbor, NY. 5/18 (2008).
8. 中山敬一: 細胞周期とアポトーシスを結ぶ p53 制御の新機構 : CHD8/ヒストン H1 によるエピジェネティックコントロール. ***第 72 回日本生化学会中部支部例会・シンポジウム***. (シンポジウム) 岐阜. 5/24 (2008).
9. 白根道子, 中山敬一: Protrudin ノックアウトマウスにおける痙性麻痺とスフィンゴ脂質結合による神経グリア相互作用への関与. ***第 60 回日本細胞生物学会大会***. (ミニシンポジウム) 横浜. 6/29 (2008).
10. 中山敬一, 白根道子: プロトルーディンは Rab11-GDP に結合し、特定の方向へ向かう膜輸送により神経突起形成を起こす. ***第 60 回日本細胞生物学会大会***. (ワークショップ) 横浜. 6/30 (2008).
11. 中山敬一: 細胞周期と癌. ***第 19 回日本消化器癌発生学会総会***. (教育講演) 別府. 8/29 (2008).
12. 中山敬一: ノックアウトマウスを用いた細胞周期研究 : 癌の本質を探る. ***第 22 回モロシヌス研究会***. (招待講演) 東京. 9/12 (2008).
13. Nakayama, K.I.: Cell cycle control during T-cell development. ***Japan-German Immunology Seminar "International Conference on***

Immune Regulation in Health and Disease". (Invited speaker) Fukuoka. 11/5 (2008).

14. Nakayama, K.I.: Two ubiquitin ligases control cell cycle in stem, progenitor, and differentiated cells. ***The 2nd Global COE International Symposium joint with the 18th Hot Spring Harbor Symposium of Medical Institute of Bioregulation, Kyushu University "Stem Cells and Regenerative Medicine"***. (Invited speaker) Fukuoka. 11/9 (2008).
15. Nakayama, K.I.: Two F-box prtoteins Skp2 and Fbw7 control cell cycle exit and re-entry. ***ZOMES V: The Fifth International Symposium on the COP9 signalosome, Proteasome, and eIF3: At the interface between signaling & proteolysis***. (Invited speaker) Yokohama. 11/12 (2008).
16. 松本有樹修, 洲崎悦生, 小野山一郎, 中山敬一: 細胞周期ブレーキ因子 p57 は小脳形成に必須の役割を担う：p57 コンディショナルノックアウトマウスからの知見. ***第 31 回日本分子生物学会年会***. (一般口頭発表) 神戸. 12/9 (2008).
17. 山田真生, 田中正和, 中山啓子, 中山敬一, 藤澤順一, 三輪正直: DNA 損傷による中心体増幅を起こす経路の特定. ***第 31 回日本分子生物学会年会***. 神戸. 12/9 (2008).
18. 細田將太郎, 白根道子, 中山敬一: Protrudin の効果的な突起伸長作用には VAMP-associated protein (VAP)が必要である. ***第31回日本分子生物学会年会***. (一般口頭発表) 神戸. 12/10 (2008).
19. 雑賀徹, 多田敬典, 岡野栄之, 中山敬一: 新規ユビキチン化酵素複合体 Fbxo45-PAM は神経発達に重要な役割を果たす. ***第 31 回日本分子生物学会年会***. 神戸. 12/10 (2008).
20. 山田政典, 小野山一郎, 恒松良祐, 中山敬一: ユビキチン-プロテアソーム系によるサイクリン D1 の分解における SCF 複合体の機能解析. ***第 31 回日本分子生物学会年会***. 神戸. 12/10 (2008).
21. 石川善則, 奥山隆平, 小野山一郎, 青山慧, 中山敬一, 中山啓子: ユビキチンリガーゼ SCF は表皮角化細胞において増殖と分化を抑制する. ***第 31 回日本分子生物学会年会***. 神戸. 12/10 (2008).
22. 押川清孝, 中川直, 松本雅記, 中山敬一: ユビキチンリガーゼ欠損マウスを用いたユビキチン化標的タンパク質同定法の構築. ***第 31 回日本分子生物学会年会***. 神戸. 12/11 (2008).
23. 遠藤彬則, 山本章嗣, 松本雅記, 中山敬一, 稲田利文, 喜多村直実, 駒田雅之: 脱ユビキチン化酵素 USP36 による核小体機能の制御. ***第 31 回日本分子生物学会年会***. 神戸. 12/11 (2008).
24. 青山慧, 石川善則, 小野山一郎, 中山敬一, 中山啓子: ユビキチ

ンリガーゼ SCF/Fbxw7 は B リンパ球の分化・生存の制御因子である. ***第31 回日本分子生物学会年会***. (一般口頭発表) 神戸. 12/11 (2008).

25. 洲崎悦生, 中山啓子, 中山敬一: ノックインマウスを用いた p27 と p57 の機能的類似性と特異性の検討. ***第 31 回日本分子生物学会年会***. (一般口頭発表) 神戸. 12/11 (2008).

26. 弓本佳苗, 松本雅記, 中山敬一: 定量的プロテオミクスを用いた細胞周期を制御するユビキチンリガーゼ基質の網羅的同定. ***第 31 回日本分子生物学会年会***. (一般口頭発表) 神戸. 12/11 (2008).

27. 石田典子, 家村俊一郎, 夏目徹, 中山敬一, 中山啓子: 新規 RING-finger タンパク質は NAP1L1 のユビキチン化を介して細胞増殖を制御する. ***第 31 回日本分子生物学会年会***. (一般口頭発表) 神戸. 12/11 (2008).

28. 中山敬一, 弓本佳苗, 押川清孝, 松本雅記: プロテオミクスが拓く細胞周期研究の新地平: リン酸化とユビキチン化に関する網羅的解析. ***第 31 回日本分子生物学会年会***. (シンポジウム) 神戸. 12/11 (2008).

29. 筑波隆幸, 柳川三千代, 門脇知子, 岡本美子, 岡元邦彰, 中山敬一, 山本健二: カテプシン E 欠損はオートファージの低下とそれに伴うミトコンドリア機能異常と酸化ストレスを引き起こす. ***第 31 回日本分子生物学会年会***. 神戸. 12/12 (2008).

30. 白根道子, 細田將太郎, 中山敬一: Protrudin の脂質統合を介した神経機能制御への関与 : Protrudin ノックアウトマウスからの知見. ***第31 回日本分子生物学会年会***. (シンポジウム) 神戸. 12/12 (2008).

31. 中山敬一: ユビキチン化による細胞周期のコントロールと胸腺腫瘍. ***第 28 回日本胸腺研究会***. (特別講演) 福岡. 2/14 (2009).

32. Matsumoto, A., Susaki, E., Onoyama, I., Nakayama, K.I.: Cell cycle inhibitor p57 is essential for neural development. ***3rd Global-COE International Symposium: Stem Cells and Regenerative Medicine***. (Invited speaker) Singapore. 2/16 (2009).

33. Nishiyama, M., Nakayama, K.I.: Epigenetic control of p53 function by CHD8 through recruitment of histone H1. ***3rd Global-COE International Symposium: Stem Cells and Regenerative Medicine***. (Invited speaker) Singapore. 2/16 (2009).

34. 中山敬一: クロマチンリモデリングによるアポトーシスの回避機構. ***平成 20 年度生理学研究所研究会 : 細胞死研究の多面的、包括的理解に向けて***. (招待講演) 岡崎. 3/17 (2009).

H. 知的財産権の出願・登録状況

1. 特許取得

該当なし

2. 実用新案登録
該当なし

3. その他
該当なし

別添４　研究成果の刊行に関する一覧表

Genome-wide DNA methylation profiles in both precancerous conditions and clear cell renal cell carcinomas are correlated with malignant potential and patient outcome

Eri Arai, Saori Ushijima, Hiroyuki Fujimoto, Fumie Hosoda, Tatsuhiro Shibata, Tadashi Kondo, Sana Yokoi, Issei Imoto, Johji Inazawa, Setsuo Hirohashi, and Yae Kanai

Carcinogenesis, Vol. 30, No.2, pp.214–221, 2009.

Identification of a Predictive Biomarker for Hematologic Toxicities of Gemcitabine

Junichi Matsubara, Masaya Ono, Ayako Negishi, Hideki Ueno, Takuji Okusaka, Junji Furuse, Koh Furuta, Emiko Sugiyama, Yoshiro Saito, Nahoko Kaniwa, Junichi Sawada, Kazufumi Honda, Tomohiro Sakuma, Tsutomu Chiba, Nagahiro Saijo, Setsuo Hirohashi, and Tesshi Yamada

Journal of Clinical Oncology, in press.

Proteomic Profiling Reveals the Prognostic Value of Adenomatous Polyposis Coli–End-Binding Protein 1 in Hepatocellular Carcinoma

Tatsuya Orimo, Hidenori Ojima, Nobuyoshi Hiraoka, Shigeru Saito, Tomoo Kosuge, Tatsuhiko Kakisaka, Hideki Yokoo, Kazuaki Nakanishi, Toshiya Kamiyama, Satoru Todo, Setsuo Hirohashi, and Tadashi Kondo

Hepatology, Vol. 48, No. 6, pp. 1851-1863, 2008.

Common and specific roles of the related CDK inhibitors p27 and p57 revealed by a knock-in mouse model

Etsuo Susakia, Keiko Nakayam, Lili Yamasaki, and Keiichi I. Nakayama

PNAS, in press.

CHD8 suppresses p53-mediated apoptosis through histone H1 recruitment during early embryogenesis

Masaaki Nishiyama, Kiyotaka Oshikawa, Yu-ichi Tsukada, Tadashi Nakagawa, Shun-ichiro Iemura, Tohru Natsume, Yuhong Fan, Akira Kikuchi, Arthur I. Skoultchi, and Keiichi I. Nakayama

Nature Cell Biology, in press.

Carcinogenesis vol.30 no.2 pp.214–221, 2009
doi:10.1093/carcin/bgn268
Advance Access publication November 26, 2008

Genome-wide DNA methylation profiles in both precancerous conditions and clear cell renal cell carcinomas are correlated with malignant potential and patient outcome

Eri Arai, Saori Ushijima, Hiroyuki Fujimoto[1], Fumie Hosoda[2], Tatsuhiro Shibata[2], Tadashi Kondo[3], Sana Yokoi[4], Issei Imoto[4], Johji Inazawa[4], Setsuo Hirohashi and Yae Kanai*

Pathology Division, National Cancer Center Research Institute, 5-1-1 Tsukiji, Chuo-ku, Tokyo 104-0045, Japan, [1]Urology Division, National Cancer Center Hospital, Tokyo 104-0045, Japan, [2]Cancer Genomics Project and [3]Proteome Bioinformatics Project, National Cancer Center Research Institute, Tokyo 104-0045, Japan and [4]Department of Molecular Cytogenetics, Medical Research Institute and School of Biomedical Science, Tokyo Medical and Dental University, Tokyo 113-8510, Japan

*To whom correspondence should be addressed. Tel: +81 3 3542 2511; Fax: +81 3 3248 2463; Email: ykanai@ncc.go.jp

To clarify genome-wide DNA methylation profiles during multistage renal carcinogenesis, bacterial artificial chromosome array-based methylated CpG island amplification (BAMCA) was performed. Non-cancerous renal cortex tissue obtained from patients with clear cell renal cell carcinomas (RCCs) (N) was at the precancerous stage where DNA hypomethylation and DNA hypermethylation on multiple bacterial artificial chromosome (BAC) clones were observed. By unsupervised hierarchical clustering analysis based on BAMCA data for their N, 51 patients with clear cell RCCs were clustered into two subclasses, Clusters A_N ($n = 46$) and B_N ($n = 5$). Clinicopathologically aggressive clear cell RCCs were accumulated in Cluster B_N, and the overall survival rate of patients in Cluster B_N was significantly lower than that of patients in Cluster A_N. By unsupervised hierarchical clustering analysis based on BAMCA data for their RCCs, 51 patients were clustered into two subclasses, Clusters A_T ($n = 43$) and B_T ($n = 8$). Clinicopathologically aggressive clear cell RCCs were accumulated in Cluster B_T, and the overall survival rate of patients in Cluster B_T was significantly lower than that of patients in Cluster A_T. Multivariate analysis revealed that belonging to Cluster B_T was an independent predictor of recurrence. Cluster B_N was completely included in Cluster B_T, and the majority of the BAC clones that significantly discriminated Cluster B_N from Cluster A_N also discriminated Cluster B_T from Cluster A_T. In individual patients, DNA methylation status in N was basically inherited by the corresponding clear cell RCC. DNA methylation alterations in the precancerous stage may generate more malignant clear cell RCCs and determine patient outcome.

Introduction

It is known that DNA hypomethylation results in chromosomal instability as a result of changes in chromatin structure and that DNA hypermethylation of CpG islands silences tumor-related genes in cooperation with histone modification in human cancers (1–5). Accumulating evidence suggests that alterations of DNA methylation are involved even in the early and the precancerous stages (6,7). On the other hand, in patients with cancers, aberrant DNA methylation is significantly associated with poorer tumor differentiation, tumor aggressiveness and poor prognosis (6,7). Therefore, alterations of DNA methylation may play a significant role in multistage carcinogenesis and can become an indicator for carcinogenetic risk estimation and a biological predictor of poor prognosis in patients with cancers. Recently developed array-based technology for accessing genome-wide DNA methylation status (8–10) is now mainly used to identify tumor-related genes silenced by DNA methylation in human cancers. Subclassification of cancers based on DNA methylation status, which may reflect the distinct epigenetic pathways of carcinogenesis, and DNA methylation profiles, which could become the optimum indicator for carcinogenetic risk estimation and prediction of patient outcome, should be further explored in each organ using array-based approaches.

With respect to renal carcinogenesis, we have reported that accumulation of DNA methylation on C-type CpG islands occurs in a cancer-specific but not age-dependent manner (11), even in non-cancerous renal tissue samples obtained from patients with clear cell renal cell carcinomas (RCCs) (6,7,12). Although precancerous conditions in the kidney have been rarely described, from the viewpoint of altered DNA methylation, non-cancerous renal tissues obtained from patients with clear cell RCCs are considered to already be at the precancerous stage in spite of showing no remarkable histological changes and lacking association with chronic inflammation and persistent infection with viruses or other pathogenic microorganisms. Surprisingly, accumulation of DNA methylation on C-type CpG islands in such non-cancerous renal tissues has been shown to be significantly correlated with higher histological grades of the corresponding clear cell RCCs developing in individual patients (6,7,12). However, since in the previous study we examined DNA methylation status on only a restricted number of CpG islands (12), we were unable to conclude that genome-wide DNA methylation alterations in precancerous conditions generate more malignant RCCs. In the previous study, accumulation of DNA methylation on C-type CpG islands in clear cell RCCs themselves was significantly correlated with tumor aggressiveness and poorer patient outcome (12). However, we were unable to conclude that the examined C-type CpG islands are the optimum prognostic indicator for patients with clear cell RCCs.

In this study, in order to clarify genome-wide DNA methylation profiles during multistage renal carcinogenesis, we performed bacterial artificial chromosome array-based methylated CpG island amplification (BAMCA) (13–15) using a microarray of 4361 bacterial artificial chromosome (BAC) clones (16) in normal renal cortex tissue samples, non-cancerous renal cortex tissue samples obtained from patients with clear cell RCC and the corresponding clear cell RCCs.

Abbreviations: BAC, bacterial artificial chromosome; BAMCA, bacterial artificial chromosome array-based methylated CpG island amplification; RCC, renal cell carcinoma; TNM, tumor–node–metastasis.

Materials and methods

Patients and tissue samples

Paired specimens of cancerous tissue (T1–T51) and corresponding non-cancerous renal cortex tissue showing no remarkable histological changes (N1–N51) were obtained from materials surgically resected from 51 patients (RCC1–RCC 51) with primary clear cell RCC. These patients did not receive preoperative treatment and underwent nephrectomy in 1999–2006 at the National Cancer Center Hospital, Tokyo, Japan. There were 34 men and 17 women with a mean (±SD) age of 59 ± 10 years (range 31–81 years). Histological diagnosis was made in accordance with the World Health Organization classification (17). All the tumors were graded on the basis of

previously described criteria (18) and classified according to the pathological tumor–node–metastasis (TNM) classification (19). The criteria for macroscopic configuration of RCC (12) followed those established for hepatocellular carcinoma: type 3 (contiguous multinodular type) hepatocellular carcinomas show poorer histological differentiation and a higher incidence of intrahepatic metastasis than type 1 (single nodular type) and type 2 (single nodular type with extranodular growth) hepatocellular carcinomas (20). The presence or absence of vascular involvement was examined microscopically on slides stained with hematoxylin–eosin and elastica van Gieson. The presence or absence of tumor thrombi in the main trunk of the renal vein was examined macroscopically. RCC is usually encapsulated by a fibrous capsule and well demarcated and hardly ever contains fibrous stroma between cancer cells (panel T in Figure 1A). Therefore, we were able to obtain cancer cells of high purity from surgical specimens, avoiding contamination with both non-cancerous epithelial cells and stromal cells.

For comparison, eight normal renal cortex tissue samples (C1–C8) were obtained from materials surgically resected from eight patients without any primary renal tumor. These patients included five men and three women with a mean (±SD) age of 61 ± 12 years (range 47–81 years). Six of these patients underwent nephroureterectomy for urothelial carcinomas of the ureter, and the other two patients underwent nephrectomy with resection of retroperitoneal sarcoma around the kidney.

High-molecular weight DNA from these fresh frozen tissue samples was extracted using phenol–chloroform, followed by dialysis. Because DNA methylation status is known to be organ specific (21), the reference DNA for analysis of the developmental stages of clear cell RCC should be obtained from the renal cortex and not from other organs or peripheral blood. Therefore, a mixture of normal renal cortex tissue DNA obtained from six male patients (C9–C14) without any primary renal tumor was used as a reference for analyses of male test DNA samples, and a mixture of normal renal cortex tissue DNA obtained from three female patients (C15–C17) without any primary renal tumor was used as a reference for analyses of female test DNA samples.

This study was approved by the Ethics Committee of the National Cancer Center, Tokyo, Japan.

BAMCA

DNA methylation status was analyzed by BAMCA using a custom-made array (MCG Whole Genome Array-4500) harboring 4361 BAC clones throughout chromosomes 1–22 and X and Y (16), as described previously (13–15). Briefly, 5 μg aliquots of test or reference DNA were first digested with 100 U of methylation-sensitive restriction enzyme SmaI and subsequently with 20 U of methylation-insensitive XmaI. Adapters were ligated to XmaI-digested sticky ends, and polymerase chain reaction was performed with an adapter primer set. Test and reference polymerase chain reaction

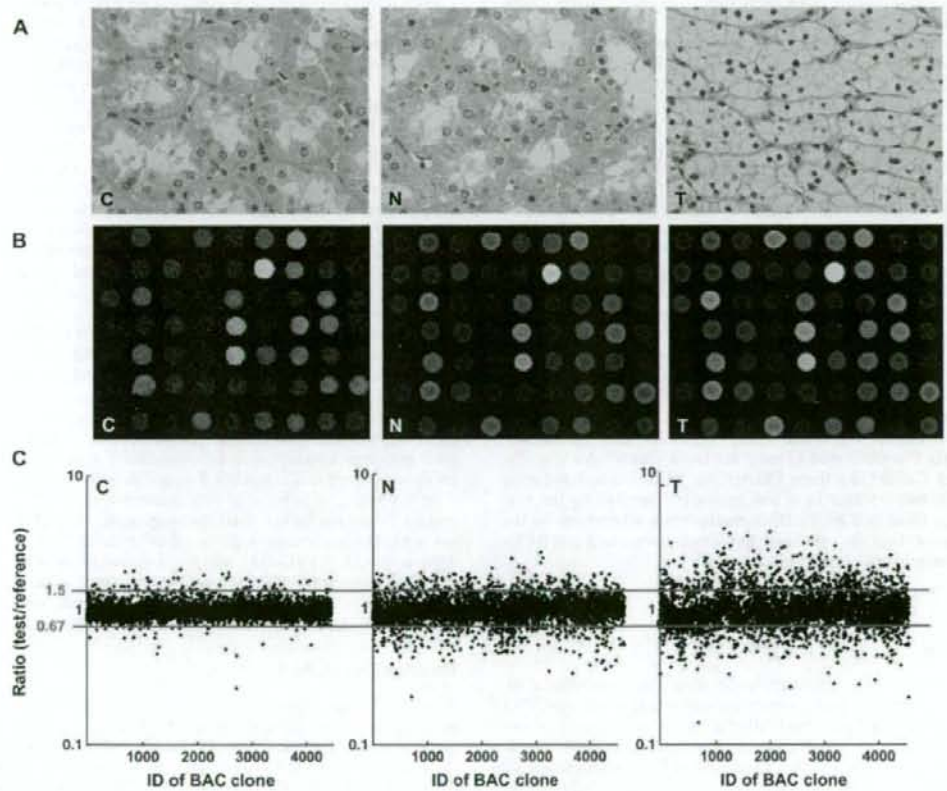

Fig. 1. DNA methylation alterations during multistage renal carcinogenesis. (**A**) Microscopic view of normal renal cortex tissue obtained from a patient without any primary renal tumor (C), non-cancerous renal cortex tissue obtained from a patient with clear cell RCC (N) and clear cell RCC (T). N shows no remarkable histological changes compared with C, i.e. no cytological or structural atypia is evident in N. Since T hardly ever contains fibrous stroma between cancer cells, we were able to obtain cancer cells of high purity, avoiding contamination with stromal cells. Hematoxylin–eosin staining. Original magnification ×20. (**B**) Scanned array images yielded by BAMCA in C, N and T. Test and reference DNA labeled with Cy3 and Cy5 was cohybridized, respectively. (**C**) Scattergrams of the signal ratios (test signal:reference signal) yielded by BAMCA in C, N and T. In all eight C samples (C1–C8), the signal ratios of 97% of BAC clones were between 0.67 and 1.5 (red bars). Therefore, in N and T, DNA methylation status corresponding to a signal ratio of <0.67 and >1.5 was defined as DNA hypomethylation and DNA hypermethylation on each BAC clone compared with C, respectively. Even though N did not show any remarkable histological changes compared with C [panels C and N in (A)], many BAC clones showed DNA hypomethylation or hypermethylation. In T, more BAC clones showed DNA hypomethylation or hypermethylation, and the degree of DNA hypomethylation and hypermethylation, i.e. deviation of the signal ratio from 0.67 or 1.5, was increased in comparison with N.

products were labeled by random priming with Cy3- and Cy5-dCTP (GE Healthcare, Buckinghamshire, UK), respectively, using a BioPrime array CGH genomic labeling system (Invitrogen, Carlsbad, CA) and precipitated together with ethanol in the presence of Cot-I DNA. The mixture was applied to array slides and incubated at 43°C for 72 h. Arrays were scanned with a GenePix Personal 4100A (Axon Instruments, Foster City, CA) and analyzed using GenePix Pro 5.0 imaging software (Axon Instruments) and Acue 2 software (Mitsui Knowledge Industry, Tokyo, Japan). The signal ratios were normalized in each sample to make the mean signal ratios of all BAC clones 1.0.

Statistics

Differences in the average number of BAC clones that showed DNA methylation alterations (DNA hypomethylation and hypermethylation) between non-cancerous renal cortex tissue samples obtained from patients with clear cell RCCs, and the clear cell RCCs themselves, were analyzed using the Mann–Whitney *U*-test. Differences at $P < 0.05$ were considered significant. Two-dimensional unsupervised hierarchical clustering analysis of the patients with clear cell RCCs and the BAC clones based on the signal ratios (test signal: reference signal) obtained by BAMCA in non-cancerous renal cortex tissue samples and those in clear cell RCCs were performed using the Expressionist software program (Gene Data, Basel, Switzerland). Correlations between the subclassification of patients with clear cell RCCs yielded by the unsupervised hierarchical clustering based on DNA methylation status of non-cancerous renal cortex tissue samples (Clusters A_N and B_N) and clinicopathological parameters of the corresponding clear cell RCCs were analyzed using chi-square test. Correlations between the subclassification of patients yielded by the unsupervised hierarchical clustering based on DNA methylation status in clear cell RCCs (Clusters A_T and B_T) and clinicopathological parameters of the RCCs themselves were analyzed using chi-square test. Survival curves of patients belonging to Clusters A_N versus B_N and Clusters A_T versus B_T were calculated by the Kaplan–Meier method, and the differences were compared by the Log-rank test. The Cox proportional hazards multivariate model was used to examine the prognostic impact of the subclassification of patients based on the DNA methylation status of their clear cell RCCs (Clusters A_T and B_T), histological grade, macroscopic configuration, vascular involvement and renal vein tumor thrombi. Differences at $P < 0.05$ were considered significant. BAC clones whose signal ratios were significantly different between Clusters A_N and B_N and Clusters A_T and B_T were each identified by Wilcoxon test ($P < 0.01$).

Results

DNA methylation alterations in samples of both cancerous and non-cancerous renal cortex tissue obtained from patients with clear cell RCCs

Figure 1B and C shows examples of scanned array images and scattergrams of the signal ratios (test signal:reference signal), respectively, for normal renal cortex tissue from a patient without any primary renal tumor and both non-cancerous renal cortex tissue and cancerous tissue from a patient with clear cell RCC. In all normal renal cortex tissue samples (C1–C8), the signal ratios of 97% of the BAC clones were between 0.67 and 1.5 (red bars in Figure 1C). Therefore, in non-cancerous renal cortex tissue obtained from patients with clear cell RCCs and the clear cell RCCs themselves, DNA methylation status corresponding to a signal ratio of <0.67 and >1.5 was defined as DNA hypomethylation and DNA hypermethylation of each BAC clone compared with normal renal cortex tissue, respectively. In samples of non-cancerous renal cortex tissue obtained from patients with clear cell RCCs (N1–N51), many BAC clones showed DNA hypomethylation or DNA hypermethylation (panel N of Figure 1C). In clear cell RCCs themselves (T1–T51), more BAC clones showed DNA hypomethylation or DNA hypermethylation, and the degree of DNA hypomethylation and DNA hypermethylation, i.e. deviation of the signal ratio from 0.67 or 1.5, was increased in comparison with non-cancerous renal cortex tissue samples obtained from patients with clear cell RCCs (panel T of Figure 1C). The average number of BAC clones showing DNA hypomethylation increased significantly from non-cancerous renal cortex tissue samples obtained from patients with clear cell RCCs (93 ± 75) to clear cell RCCs (142 ± 74, $P = 0.0002$). The average number of BAC clones showing DNA hypermethylation also increased significantly in a similar manner (83 ± 73–123 ± 786, $P = 0.004$).

Unsupervised hierarchical clustering of patients with clear cell RCCs based on DNA methylation status of non-cancerous renal cortex tissue samples

By two-dimensional unsupervised hierarchical clustering analysis based on BAMCA data (signal ratios) for non-cancerous renal cortex tissue samples, the 51 patients with clear cell RCCs were clustered into two subclasses, Clusters A_N and B_N, which contained 46 and 5 patients, respectively (Figure 2A).

Table IA shows the clinicopathological parameters of clear cell RCCs of patients belonging to Clusters A_N and B_N. The corresponding clear cell RCCs of patients in Cluster B_N showed more frequent macroscopically evident multinodular (type 3) growth, vascular involvement and renal vein tumor thrombi and showed higher pathological TNM stages than those in Cluster A_N. Figure 2B shows the Kaplan–Meier survival curves of patients belonging to Clusters A_N and B_N. The period covered ranged from 88 to 2801 days (mean, 1679 days). Three (60%) of the patients in Cluster B_N died of recurrent RCC, whereas only one (2%) of the patients in Cluster A_N died. The overall survival rate of patients in Cluster B_N was significantly lower than that of patients in Cluster A_N (Figure 2B).

Although Cluster A_N was divided into three subclusters, A_{N1} ($n = 3$), A_{N2} ($n = 19$) and A_{N3} ($n = 24$) (Figure 2A), there were no significant correlations between these subclusters and any of the clinicopathological parameters examined (data not shown). Even when unsupervised hierarchical clustering was performed separately, based not on signal ratios but on the presence or absence of DNA hypomethylation and the presence or absence of DNA hypermethylation, the majority of patients in Cluster B_N were clustered into the same subclass (supplementary Figure S1A and B is available at *Carcinogenesis* Online).

Wilcoxon test ($P < 0.01$) revealed that the signal ratios of 1143 BAC clones in non-cancerous renal cortex tissue differed significantly between Clusters A_N and B_N: e.g. patients belonging to Cluster B_N were completely discriminated from patients in Cluster A_N by the DNA methylation status of samples of non-cancerous renal cortex tissue for representative BAC clones (Cluster A_N versus Cluster B_N in Figure 3A) out of the 1143 BAC clones.

Unsupervised hierarchical clustering based on DNA methylation status of clear cell RCCs

Two-dimensional unsupervised hierarchical clustering analysis based on BAMCA data (signal ratios) for clear cell RCCs was able to group 51 patients into two subclasses, Clusters A_T and B_T, which contained 43 and eight patients, respectively (Figure 2C).

Table IB shows the clinicopathological parameters of clear cell RCCs of patients belonging to Clusters A_T and B_T. Clear cell RCCs in Cluster B_T showed more frequent vascular involvement and renal vein tumor thrombi and showed higher pathological TNM stages than those in Cluster A_T. Figure 2D shows the Kaplan–Meier survival curves of patients belonging to Clusters A_T and B_T. Three (37.5%) of the patients in Cluster B_T died due to recurrent RCCs, whereas only one (2.3%) of the patients in Cluster A_T died. The overall survival rate of patients in Cluster B_T was significantly lower than that of patients in Cluster A_T (Figure 2D). Multivariate analysis revealed that our clustering was a predictor of recurrence and was independent of histological grade, macroscopic configuration, vascular involvement and renal vein tumor thrombi (Table II).

Although Cluster A_T was divided into four subclusters, A_{T1} ($n = 8$), A_{T2} ($n = 12$), A_{T3} ($n = 13$) and A_{T4} ($n = 10$) (Figure 2B), there were no significant correlations between these subclusters and any of the clinicopathological parameters examined (data not shown). Even when unsupervised hierarchical clustering was performed separately, based not on signal ratios but on the presence or absence of DNA hypomethylation and the presence or absence of DNA hypermethylation, the majority of patients in Cluster B_T were clustered into the same subclass (supplementary Figure S1C and D is available at *Carcinogenesis* Online).

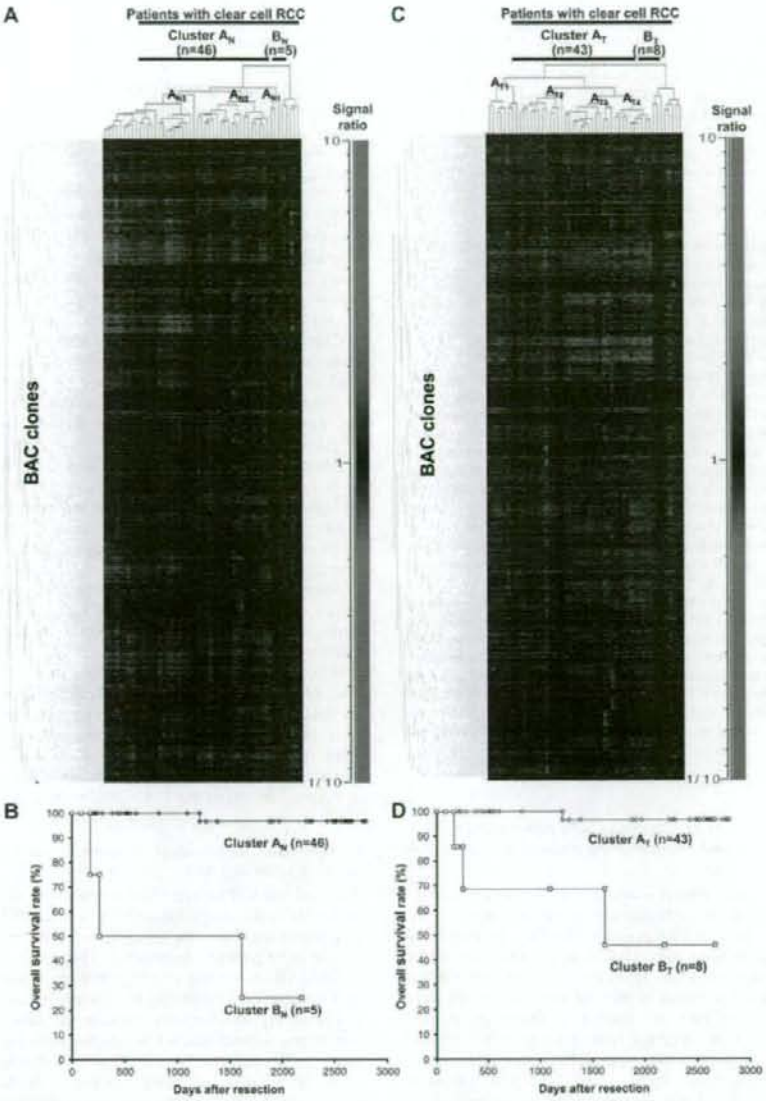

Fig. 2. Two-dimensional unsupervised hierarchical clustering analysis based on BAMCA data (signal ratios) in non-cancerous renal cortex tissue samples showing no remarkable histological changes (A) and clear cell RCCs (C) and Kaplan–Meier survival curves of patients with clear cell RCCs (B and D). (**A**) Fifty-one patients with clear cell RCC were hierarchically clustered into two subclasses, Clusters A_N ($n = 46$) and B_N ($n = 5$), based on DNA methylation status of their non-cancerous renal cortex tissue samples. DNA hypomethylation, normomethylation (DNA methylation status corresponding to a signal ratio of between 0.67 and 1.5) and hypermethylation on each BAC clone are shown in green, black and red, respectively. The signal ratio is shown in the color range maps. The cluster trees for patients and BAC clones are shown at the top and left of the panel, respectively. (**B**) The overall survival rate of patients in Cluster B_N (square) defined on the basis of DNA methylation status in their non-cancerous renal cortex tissue samples was significantly lower than that of patients in Cluster A_N (circle) ($P = 0.0000000613$, Log-rank test). (**C**) Fifty-one patients were hierarchically clustered into two subclasses, Clusters A_T ($n = 43$) and B_T ($n = 8$), based on the DNA methylation status of their clear cell RCCs. (**D**) The overall survival rate of patients in Cluster B_T (square) defined on the basis of DNA methylation status in their clear cell RCCs was significantly lower than that of patients in Cluster A_T (circle) ($P = 0.0000413$, Log-rank test).

Wilcoxon test ($P < 0.01$) revealed that the signal ratios of 1111 BAC clones in clear cell RCCs were differed significantly between Clusters A_T and B_T. In particular, patients belonging to Cluster B_T were completely discriminated from patients belonging to Cluster A_T based on the DNA methylation status of 14 BAC clones (Cluster A_T versus Cluster B_T in Figure 3A). In other words, DNA methylation status of the 14 BAC clones was able to determine whether or not patients in this cohort belonged to Cluster B_T, a significant prognostic indicator, with a sensitivity and specificity of 100% using the cutoff values shown in Figure 3A and supplementary Table

Table I. Correlation between the subclassification of patients based on DNA methylation status and the clinicopathological parameters of clear cell RCCs

(A) Clusters A_N and B_N based on DNA methylation status in non-cancerous renal cortex tissue samples				
Clinicopathalogical parameters of the corresponding clear cell RCCs developing in individual patients		Patients with clear cell RCCs		P^a
		Cluster A_N (n = 46)	Cluster B_N (n = 5)	
Macroscopic finding	Type 1	26	1	0.0248
	Type 2	10	0	
	Type 3	10	4	
Vascular involvement	Negative	38	0	0.0005
	Positive	8	5	
Renal vein tumor thrombi	Negative	41	1	0.0017
	Positive	5	4	
Pathological TNM stage	Stage I	29	0	0.0195
	Stage II	1	0	
	Stage III	13	3	
	Stage IV	3	2	
(B) Clusters A_T and B_T based on DNA methylation status in clear cell RCCs				
Clinicopathalogical parameters of clear cell RCCs		Patients with clear cell RCCs		P^a
		Cluster A_T (n = 43)	Cluster B_T (n = 8)	
Macroscopic finding	Type 1	24	3	NS[b]
	Type 2	9	1	
	Type 3	10	4	
Vascular involvement	Negative	35	3	0.0297
	Positive	8	5	
Renal vein tumor thrombi	Negative	38	4	0.0349
	Positive	5	4	
Pathological TNM stage	Stage I	27	2	0.0263
	Stage II	1	0	
	Stage III	13	3	
	Stage IV	2	3	

[a]Chi-square test.
[b]Not significant.

SI (available at *Carcinogenesis* Online). DNA methylation status of the 70 BAC clones, including the above 14 BAC clones, was able to determine whether or not the patients in this cohort belonged to Cluster B_T, with a sensitivity of 100% and a specificity of 90 or >90%, using the cutoff values shown in supplementary Table SI (available at *Carcinogenesis* Online).

Comparison between DNA methylation profiles of non-cancerous renal tissue and those of corresponding clear cell RCC

Patients RCC1–RCC5 and patients RCC1–RCC8 were identified as belonging to Clusters B_N and B_T, respectively, by unsupervised hierarchical clustering based on BAMCA data for non-cancerous renal cortex tissue samples and clear cell RCCs. Namely, Cluster B_N (n = 5) was completely included in Cluster B_T (n = 8). The 724 BAC clones, the majority of the 1143 BAC clones significantly discriminating Cluster B_N from Cluster A_N, also discriminated Cluster B_T from Cluster A_T (Wilcoxon test, $P < 0.01$). In 311 of the 724 BAC clones, where the average signal ratio of Cluster B_N was higher than that of Cluster A_N, the average signal ratio of Cluster B_T was also higher than that of Cluster A_T without exception (Figure 3A). In 413 of the 724 BAC clones, where the average signal ratio of Cluster B_N was lower than that of Cluster A_N, the average signal ratio of Cluster B_T was also lower than that of Cluster A_T without exception (Figure 3A). Figure 3B shows the signal ratios of non-cancerous renal cortex tissue samples and clear cell RCCs for all 51 patients for a representative BAC clone (RP11-44F3). In individual patients, DNA methylation status in the non-cancerous renal cortex tissue was basically inherited by the corresponding clear cell RCC (Figure 3B).

Discussion

Many researchers in this field use arrays in which the promoter regions are enriched as probes to identify the genes methylated in cancer cells (8–10). However, the promoter regions of specific genes are not the only target of DNA methylation alterations in human cancers. DNA methylation status in genomic regions not directly participating in gene silencing, such as the edges of CpG islands, may be altered at the precancerous stage before the alterations of the promoter regions themselves occur (22). Genomic regions in which DNA hypomethylation affects chromosomal instability may not be contained in promoter arrays. Moreover, aberrant DNA methylation of large regions of chromosomes, which are regulated in a coordinated manner in human cancers due to a process of long-range epigenetic silencing, has recently attracted attention (23). Therefore, we used a custom-made BAC array (16) that may be suitable, not for focusing on specific promoter regions or individual CpG sites but for overviewing the DNA methylation status of individual large regions among all chromosomes and for subclassifying cancers by hierarchical clustering.

With respect to renal carcinogenesis, several studies of DNA methylation profiles of genes involved in specific signal pathways in clear cell RCCs, such as the p53-signaling (24) and Wnt-signaling (25) pathways, have been performed. However, to our knowledge, there have been no published data on DNA methylation profiles for all chromosomes in clear cell RCCs revealed by array-based technology. In our previous study, we showed that samples of non-cancerous renal cortex tissue from patients with clear cell RCC were already at the precancerous stage with accumulation of DNA methylation on C-type CpG islands, in spite of an absence of marked histological changes (6,7,12). In the present study, genome-wide DNA methylation alterations (both hypomethylation and hypermethylation) in samples of non-cancerous renal cortex tissue from patients with clear cell RCC were confirmed by BAMCA (panel N of Figure 1B and C). We then performed unsupervised hierarchical clustering analysis based on the genome-wide DNA methylation status of the non-cancerous renal cortex tissue samples, and as a result, 51 patients were subclassified into Clusters A_N and B_N. Corresponding clear cell RCCs showing multinodular growth, vascular involvement, renal vein tumor thrombi and higher pathological TNM stages were found to be accumulated in Cluster B_N. Although subclassification of precancerous tissue by unsupervised hierarchical clustering analysis on the basis of genome-wide DNA methylation profiles has never been performed for specific organs, our Clusters A_N and B_N can be considered clinicopathologically valid.

The significant correlation between genome-wide DNA methylation profiles of samples of non-cancerous renal cortex tissue and